

Electrochemical Properties of Silver-Nylon Fabrics

Andrew A. Marino, Visit Malakanok, and James A. Albright

Department of Orthopaedic Surgery, Louisiana State University Medical School, Shreveport, Louisiana 71130-3932

Edwin A. Deitch

Department of Surgery, Louisiana State University Medical School, Shreveport, Louisiana 71130-3932

Robert D. Specian

Department of Anatomy, Louisiana State University Medical School, Shreveport, Louisiana 71130-3932

ABSTRACT

Composites consisting of inert fiber substrates coated with metallic silver were shown to be potentially useful as a source of silver ions for infection control. Using an *in vitro* system, the ability of six silver-coated nylon fabrics to support an electric current was studied, and the resulting silver levels up to 23h after initiation of the current were measured. In four fabrics, $1.7 \mu\text{A}/\text{cm}^2$ for 16h produced fabric corrosion that prevented further current flow. Comparable changes in two other fabrics did not occur until $16 \mu\text{A}/\text{cm}^2$. At fixed current densities, the fabrics produced differing solution silver concentrations. For one fabric, the measured silver concentrations approached the theoretically predicted level. The results indicated that silver-nylon fabrics could produce antimicrobially significant silver levels at relatively low currents and voltages, and that the rate of ion production can be predicted on the basis of electrochemical considerations.

Silver compounds are used in clinical medicine because of their antiseptic properties (1). The prophylaxis of ocular infections and prevention and treatment of burnwound sepsis are two examples. Beginning in the late 19th century, metallic silver in the form of sutures and foils was used to produce bacteriostatic effects via the passive disassociation of silver from the metallic phase into tissue (2). Metallic silver continued to be used clinically until the systemic antibiotics were introduced in the 1930's.

Interest in the possible use of metallic silver as a topical antimicrobial agent developed again in the 1970's, when a series of studies showed that electrically generated silver ions inhibited the growth of bacteria and fungi (3-8). The first attempt at clinical application of this concept involved the treatment of osteomyelitis (9). To increase the area of tissue actually exposed to silver ions, silver-coated nylon fabric as well as thin silver wire were used.

The concept of applying an antiseptic agent by passing a current through a metallized fabric has clinical appeal: (i) the dose can be regulated by controlling the current; (ii) the textile characteristics of the substrate can be chosen to produce an occlusive or nonocclusive dressing, as needed; (iii) since a typical wound dressing would contain only a few milligrams of silver, the cost of the dressing would be low.

To pursue this idea, the *in vitro* electrical properties of a commercially available class of silver-coated nylon fabrics were studied. Our aim was to elucidate the electrochemical response of the fabrics under conditions that simulated actual clinical use.

Methods

Six fabrics (Swift Textile Metalizing Corporation, Hartford, Connecticut) were studied. The fabric designations and some of their physical properties are listed in Table I. The fabrics consisted of woven or knitted nylon fibers, 20-50 m diam, that had been uniformly coated with pure silver to a calculated average thickness of 0.02-0.4 m, depending on the fabric. The coating process did not affect the handling characteristics or mechanical strength of the fabrics.

For dc studies, the fabrics were prepared as annular electrodes with tabs to permit introduction of the current (Fig. 1A). The fabrics were not treated prior to use except for a brief rinse in distilled water. In most experiments, the tabs were coated with an insulating material (Paraplast, Lancer, St. Louis, Missouri) to prevent wick action.

The Paraplast was applied to the tabs at 56°C and allowed to harden at room temperature; it did not affect the pertinent physical properties of the fabrics. In some cases, to increase the current per unit area of the fabric, part of the annular ring was removed (Fig. 1A). The fabrics were operated as anodes against silver-wire cathodes (23 cm of 0.5 mm diam silver wire) in the configuration shown in Fig. 1B. The cathode material and configuration were chosen for convenience, and they had no specific effect on events within the anodic chambers which did not vary when stainless steel, copper, or silver-nylon fabrics (surface area 0.16-60 cm^2) were used.

Silver measurements were made by atomic absorption spectroscopy using standard methods (10). Briefly, aliquots of the solution under study, after dilution if needed, were directly aspirated into an air-acetylene flame. Silver concentrations were determined by absorbance measurements (Perkin-Elmer 306, with a silver hollow-cathode lamp) with the use of standard curves generated by adding known concentrations of silver to the same medium as the test solution. The 328.0 nm resonance line of silver was used, and all measurements were made in triplicate and the results averaged.

Current was applied using a variable power supply (EICO 10645) and measured with an electrometer (Keithley, 610C) or a digital multimeter (Beckman 3020) (see Fig. 1). A second such multimeter was used for resistance

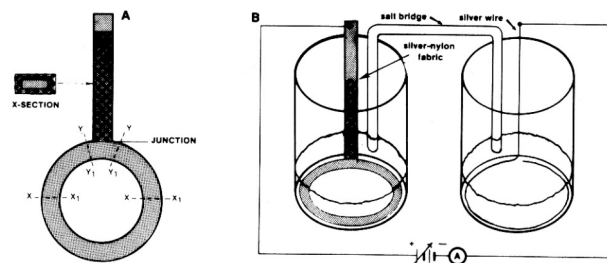


Fig. 1. The experimental system. (A) Geometry of the annular electrode. Two additional electrode geometries were used in some measurements. The semi-annular electrode produced by cutting the fabric at X-X₁ (and discarding the distal portion); the tab electrode produced by cutting the fabric at Y-Y₁. The surface areas were, respectively, 19, 9.5, 1 cm^2 . (B) For passage of current, the portion of the electrode distal to the junction was immersed in 50 ml of medium—either saline or tryptic soy broth—contained in 400 ml beakers. Electrical connection to the cathodal beaker was made via a tryptic-agar bridge.

Table I. Properties of silver-nylon fabrics

Fabric style	HRS	LRS	SN	R	4H	IT
Pattern	Weave	Weave	Knit	Knit	Knit	Knit
Cell shape	Square	Square	Square	Diamond	Hexagonal	Hexagonal
Cell size (mm)	Closed	Closed	Closed	4.8	2.5	0.76
Weight (g/m ²)	84.6	37.2	111.7	67.7	13.5	10.2
Silver content (μg/cm ²)	2545	783	4364	2371	500	371

Table II. Electrical resistance of silver-nylon fabrics as a function of immersion time in saline at 20° (upper) and 37° (lower). Average and one standard deviation (*n* = 1 weighting) of triplicate determinations. NM; not measured

Fabric style	Resistance (Ω/□)				
	Nonimmersed	1h	4h	24h	96h
HRS	1.0 ± 0.2	1.4 ± 0.5 199.7 ± 182.2	3.5 ± 2.6 558.1 ± 552.6	>20 MΩ >20 MΩ	NM >20 MΩ
LRS	1.6 ± 0.8	2.1 ± 0.5 1.8 ± 1.8	3.0 ± 0.3 1.6 ± 1.1	2.0 ± 0.7 2.0 ± 2.0	NM 2.8 ± 0.5
SN	1.2 ± 0.2	1.3 ± 0.1 1.3 ± 0.1	1.3 ± 0.1 1.6 ± 0.1	3.4 ± 0.7 >20 MΩ	NM >20 MΩ
R	0.6 ± 0.1	1.1 ± 0.1 1.0 ± 0.1	0.9 ± 0.1 1.0 ± 0.1	1.0 ± 0.1 1.0 ± 0.1	NM 1.1 ± 0.1
4H	2.5 ± 0.5	3.7 ± 0.1 4.9 ± 1.3	3.6 ± 0.3 5.2 ± 0.8	6.1 ± 1.7 10.3 ± 3.0	NM 65.1 ± 60.2
IT	1.3 ± 0.1	1.9 ± 0.1 2.2 ± 0.5	1.8 ± 0.1 2.1 ± 0.1	2.2 ± 0.2 5.2 ± 0.3	NM 1300 ± 1900

measurements. The voltages reported were the potential differences applied between the chambers; they were monitored with a high impedance voltmeter (RCA WV 510-A). For scanning electron microscopy (SEM), 1 cm squares of fabric were cut out and adhered to aluminum scanning stubs with copper-impregnated tape. The specimens were examined and photographed in an AMR 1200 scanning electron microscope at an accelerating voltage of 25 kV.

The unmetallized fabrics did not undergo detectable changes in resistance when subjected to the conditions of immersion employed in this study. The electrical changes observed are, therefore, attributed to changes in the silver coating, and not the nylon itself.

Results

The fabrics exhibited changes in surface resistance following immersion in saline (Table II). A typical current vs. time curve for fabric HRS is shown in Fig. 2. At 1V after 9-0h, the current dropped precipitously. When the average current density was increased using a semi-annular or tab anode (the total current was unchanged), the current drop-off occurred at proportionately earlier times (Table III).

For immersion times greater than 24h, the resistance between any two points on the annular portion of the

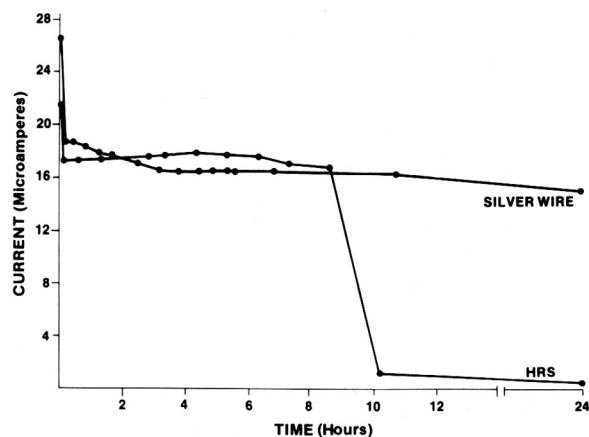


Fig. 2. Total current through HRS and silver-wire anodes: 1 V, 2-° C, in saline.

HRS anode (or between any two points, one of which was in the annular portion) was essentially infinite regardless of whether it had been used to pass current or not. But for immersion times sufficiently short that the passive disassociation of silver from the fabric did not affect the total system current, the pattern of resistance measurements was related to the current density passed through the fabric and, more particularly, to the occurrence of the dropoff phenomenon. Before the drop-off, all resistance measurements, including those having a path across the junction, were on the order of *i*D. Immediately after the drop-off, however, only resistance paths that did not cross the junction yielded low values; all paths through the junction showed essentially infinite resistance.

The sequence of measurements was repeated with IT which, unlike HRS, underwent negligible changes in resistance due to immersion in saline (Table II), and again the current drop-off was observed (Table III). Before the current drop-off occurred, all resistance measurements were on the order of 111; after the drop-off, essentially infinite resistance across the junction was again measured.

The extent of the region at the junction manifesting the electrolytic effects on surface resistance depended on

Table III. Maximum duration of current flow as a function of average current density. All measurements were made at 1V, 20°C, in saline

Fabric style	Electrode geometry	Current density (pA/cm ²)	Time to current drop-off (h)
HRS	Annular	0.85	10
	Semi-annular	1.70	5
	Tab	16	3
LRS	Annular	0.85	24
	Semi-annular	1.70	8-16
	Tab	16	2
SN	Annular	0.85	>24
	Semi-annular	1.70	>24
	Tab	16	17-23
R	Annular	0.85	>24
	Semi-annular	1.70	>24
	Tab	16	10-14
4H	Annular	0.85	21
	Semi-annular	1.70	10-14
	Tab	16	3
IT	Annular	0.85	17
	Semi-annular	1.70	10
	Tab	16	3

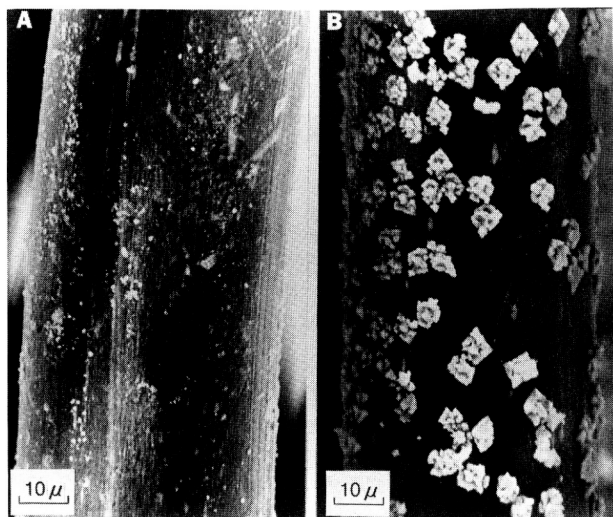


Fig. 3. Scanning electron micrograph of the junction region of IT. A: Control. B: after passage of current for 23h, 1 V, 2-°C, in saline.

electrode geometry and voltage. Generally, it was 1-3 cm², which corresponded to 10-100% of the electrode surface actually exposed to the solution.

4H and LBS exhibited behavior qualitatively similar to that of IT; they were stable (Table II) and exhibited both a current drop-off (Table III) and a corresponding high resistance in the neighborhood of the junction. B and SN were also stable, but were able to support a current for 24h for all but the highest current density (Table III).

SEM showed that the formation of surface-adhering crystals - presumed to be silver chloride - accompanied the passage of current. Figure 3, which depicts the crystal formation in the junction region of IT, is typical of the observed surface corrosion. By SEM, the density of crystal formation appeared to be greater in the junctional region compared to that in the opposite portion of the electrode (Fig. 4), but actual measurements were not performed. Al-

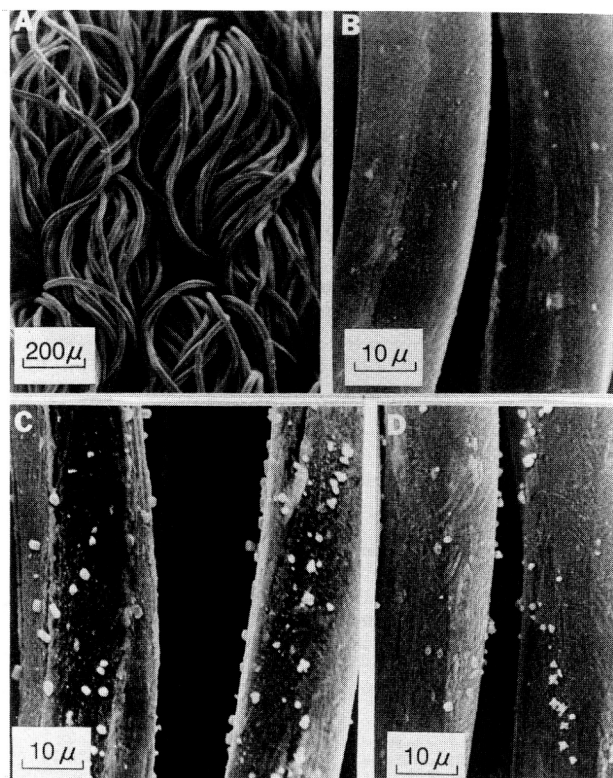


Fig. 4. Scanning electron micrograph of SN. A and B: control. C and D: after 1 V, 20°C, in saline. C: region near the junction. D: region in the most distal portion of the electrode.

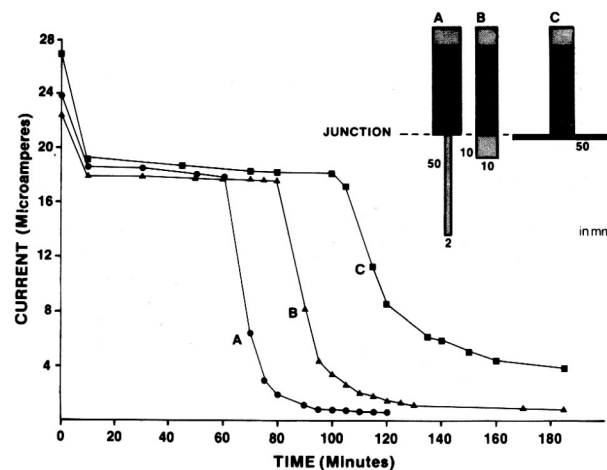


Fig. 5. Total current through HRS anodes having the same areas but differing in junction geometries. IN saline, 20°C, 1 V.

though the effect of the passage of current through the fabrics could be readily detected by SEM, there were no corresponding macroscopic changes in any of the fabrics.

To explore the role of the geometry of the junction it self when the average current density was held constant, we prepared electrodes having the same surface area but widely different junction geometries (Fig. 5). The narrowest junction exhibited both the most rapid onset of the current drop-off, and lowest base-line current. The 50 mm junction exhibited a diffuse current drop-off with the longest onset and highest base-line level. The 10 mm junction was intermediate with respect to both characteristics.

Knowledge of the electrical characteristics of the silver-nylon fabrics is important with regard to their contemplated clinical uses for infection control. Data regarding the fabrics' silver-ion releasing properties is also needed, because clinical efficacy requires tissue silver levels of 5-20 $\mu\text{g/ml}$ (6). We therefore measured the silver concentrations in tryptic soy broth (a standard medium that supports microbial growth).

The fabrics themselves did not undergo significant changes in resistance following immersion in the medium (Table IV). The silver measurements were made using annular anodes. At 1V, the total system current was approximately 22 μA (average current density: 1.2 $\mu\text{A/cm}^2$ of fabric). The silver levels released into solution by both passive disassociation and electrolysis (1 and 2V) up to 23h are shown in Table V.

Discussion

Previous work showed that BBS can be effective against micro-organisms (11); silver dissolved from the fabric's surface diffused through the medium and inhibited growth. This movement of silver has been confirmed indirectly by the present measurements of fabric resistances, which rise with immersion time, suggesting that silver ions are being liberated. It has also been confirmed by the direct measurement of silver in solution. After 23h, BBS liberated 2.6 $\mu\text{g/ml}$ of silver, which is essentially the same concentration deduced in the earlier study (11).

Table IV. Electrical resistance of silver-nylon fabrics after immersion in tryptic soy broth for 24h at 37°C. Average and one standard deviation ($n = 1$ weighting) of triplicate measurements

Fabric style	Resistance (Ω/\square) 24h
HRS	1.8 \pm 0.2
LRS	2.9 \pm 0.1
SN	1.7 \pm 0.1
R	1.0 \pm 0.1
4H	5.2 \pm 0.6
IT	2.4 \pm 0.1

Table V. Silver levels in tryptic soy broth (50m l) at 37°C. Average and one standard deviation (n = 1 weighting) of triplicate measurements at (from top to bottom in each data group) 0 (control), 1, and 2V. NM: not measured

Fabric style	Silver concentration ($\mu\text{g/ml}$)				
	1h	2h	4h	7h	23h
	<0.01	<0.01	<0.01	<0.01	<0.01
Silver wire	1.1 \pm 0.1	2.1 \pm 0.1	4.4 \pm 0.2	7.0 \pm 0.5	21.3 \pm 0.7
	1.6 \pm 0.3	3.2 \pm 0.4	6.5 \pm 2.0	9.4 \pm 1.9	26.6 \pm 6.4
	0.8 \pm 0.3	1.0 \pm 0.3	1.4 \pm 0.3	1.8 \pm 0.3	2.6 \pm 1.0
HRS	1.4 \pm 0.3	2.2 \pm 0.5	3.9 \pm 0.7	7.3 \pm 0.6	14.0 \pm 0.4
	3.1 \pm 0.1	5.3 \pm 0.6	10.2 \pm 0.6	13.2 \pm 0.1	20.9 \pm 1.3*
	0.4 \pm 0.1	0.5 \pm 0.1	0.7 \pm 0.1	1.1 \pm 0.1	1.1 \pm 0.4
LRS	1.6 \pm 0.4	2.8 \pm 0.1	6.0 \pm 0.1	10.2 \pm 0.4	21.8 \pm 0.6*
	NM	NM	NM	NM	NM
	2.3 \pm 0.2	3.0 \pm 0.2	4.4 \pm 0.4	5.8 \pm 0.6	11.5 \pm 1.2
SN	3.2 \pm 0.2	4.7 \pm 0.2	8.3 \pm 0.2	12.1 \pm 0.4	21.3 \pm 1.7
	3.4 \pm 0.3	6.4 \pm 0.6	11.2 \pm 0.7	15.2 \pm 0.9	25.0 \pm 5.2
	1.4 \pm 0.2	1.9 \pm 0.2	3.0 \pm 0.3	4.0 \pm 0.4	8.0 \pm 0.6
R	2.3 \pm 0.1	3.5 \pm 0.2	7.2 \pm 0.2	10.6 \pm 0.6	23.4 \pm 1.0
	4.2 \pm 0.2	7.9 \pm 1.6	15.4 \pm 1.2	20.7 \pm 2.1	29.6 \pm 2.5
	0.7 \pm 0.1	0.9 \pm 0.1	1.4 \pm 0.1	1.9 \pm 0.2	3.0 \pm 0.9
4H	2.5 \pm 0.6	4.3 \pm 0.6	7.9 \pm 1.2	11.8 \pm 1.7	31.6 \pm 1.7*
	4.6 \pm 0.4	8.6 \pm 0.2	17.6 \pm 0.3	23.6 \pm 0.8*	NM
	0.5 \pm 0.1	0.6 \pm 0.1	1.0 \pm 0.1	1.4 \pm 0.1	2.6 \pm 0.6
IT	2.6 \pm 0.7	4.4 \pm 0.7	7.9 \pm 0.9	12.9 \pm 0.6	33.2 \pm 1.6*
	4.8 \pm 0.2	9.4 \pm 0.1	19.3 \pm 0.2	24.5 \pm 1.3*	NM

* Current drop-off observed.

All the fabrics produced silver when immersed in the medium, and the resulting silver levels varied by about a factor of 6 during the first 8h; at 23h, the range was greater than a factor of 10 (LRS compared to SN). Silver levels produced by silver wire under identical experimental conditions were below the level of detection (0.01 $\mu\text{g/ml}$). The surface area of the silver-wire anode was 3.6 cm^2 . The geometric surface of the fabrics was 19 cm^2 , but the actual surface area varied depending on the particular fabric. Based on the fabric properties listed in Table I, and assuming a fiber diameter of 20 μm (50 μm for IT), it can be shown the actual surface area, depending on the fabric, was 0.8-22 times as great as the corresponding geometric area. Thus the fabric anodes had 4-116 times the surface area of the silver anodes. Consider SN, which is the most extreme case. It had a calculated actual surface area 22 times that of its geometric area. The area of the SN anode was, therefore, 22 x 19/3.6 116 times that of the silver-wire anode. Although there was a difference of two orders of magnitude in the surface areas, there was a difference of at least three orders of magnitude in the corresponding silver levels produced by passive disassociation (Table V). This indicated that the metallic silver coating on SN was significantly more labile than silver wire. Similar calculations for the other fabrics lead to the same conclusion.

The passage of current through the fabrics resulted in increased silver levels. When the silver levels at 1 and 2V were corrected for the base-line levels, the materials ranked as follows in decreasing order of relative electrolytic efficiency with regard to liberating silver: IT, 4H, LRS, silver wire, R, SN, HRS, at 1V up to 7h; IT, 4H, R, HRS, SN, silver wire, at 2V up to 4h. Faraday's law gives as the upper limit for silver production 4 $\mu\text{g}/\mu\text{A}\cdot\text{h}$. In Fig. 6, the range of measured silver levels produced by the fabrics and silver wire is compared to the theoretical level. IT was the most faradaic of the materials in that it produced silver levels close to the predicted values.

It is the total silver concentration that determines whether microbial growth will be inhibited. Under the conditions we employed, the threshold of such an effect (approximately 5 $\mu\text{g/ml}$) occurred after 2h at 1V and after 1h at 2V. Under different but realistic experimental conditions, this threshold could probably be achieved even more quickly.

IT was one of the most interesting of the fabrics studied. Even though it was the lightest and least-silvered fabric (Table I), it produced high silver concentrations (Table V). Its major drawback was that it was among the fabrics most prone to exhibit the current drop-off (Table III).

The current drop-off phenomenon apparently arises from the preferential liberation of silver ions at the junction zone. We know of no theoretical reason to expect that the current density would be greater near the junction, but such an occurrence would explain both the high resistance region found at the junction and the SEM observations of increased corrosion at that location.

We have shown that the fabrics will electrolytically liberate silver ions into solution, producing silver levels that would be expected to inhibit the growth of microorganisms. Studies to be published elsewhere have established this activity against gram-positive and gram-negative bacteria and fungus (12). Clinical application of the silver nylon fabrics will require attention to both the design of the electrode and its geometric relationship to the treatment site. The current drop-off phenomenon exhibited by the fabrics will probably not impede their development for clinical use.

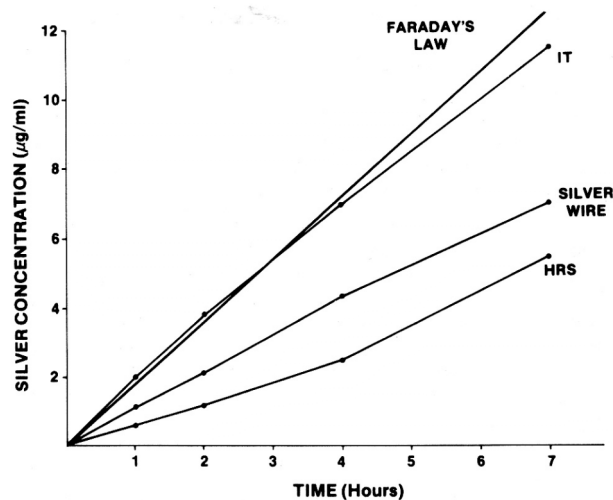


Fig. 6. Electrically produced silver concentrations (corrected for base-line levels) compared to theoretical maximum concentrations. In tryptic soy broth, 1V, 37°C.

Manuscript submitted July 9, 1984; revised manuscript received Aug. 21, 1984.

REFERENCES

1. A. G. Goodman, L. S. Goodman, and A. Gilman, "Goodman and Gilman's Pharmacological Basis of Therapeutics," 6th ed., p. 976, MacMillan Publishing Co., New York (1980).
2. W. S. Halsted, *J. Am. Med. Assoc.*, **60**, 1119 (1913).
3. S. D. Barranco, J. A. Spadaro, T. J. Berger, and R. O. Becker, *Clin. Orthop.*, **100**, 250 (1974).
4. V. W. Golubovich and I. L. Rabotnova, *Microbiology*, **43**, 948 (1974).
5. J. A. Spadaro, T. J. Berger, S. D. Barranco, S. E. Chapin, and R. O. Becker, *Antimicrob. Agents Chemother.*, **6**, 637 (1974).
6. T. J. Berger, J. A. Spadaro, S. E. Chapin, and R. O. Becker, *ibid.*, **9**, 357 (1976).
7. T. J. Berger, J. A. Spadaro, R. Bierman, S. E. Chapin, and R. O. Becker, *ibid.*, **10**, 856 (1976).
8. E. A. Thibodeau, S. L. Handelman, and B. E. Marquis, *J. Dent. Res.*, **57**, 922 (1978).
9. R. O. Becker and J. A. Spadaro, *J. Bone Joint Surg.*, **60A**, 871 (1978).
10. D. G. Van Ormer, in "CRC Handbook of Spectrophotometric Data of Drugs," I. Sunshine, Editor, p. 349, CRC Press, Boca Raton, FL (1980).
11. E. A. Deitch, A. A. Marino, T. E. Gillespie, and J. A. Albright, *Antimicrob. Agents Chemother.*, **23**, 356 (1983).
12. A. A. Marino, E. A. Deitch, V. Malakanok, J. A. Albright, and R. E. Specian, *J. Biol. Phys.*, To be published.